



Published in final edited form as:

Chem Commun (Camb). 2016 April 14; 52(29): 5136–5139. doi:10.1039/c6cc01508e.

Discovery of a ^{19}F MRI sensitive salinomycin derivative with high cytotoxicity towards cancer cells

Qiuyan Shi^a, Yu Li^a, Shaowei Bo^a, Xiaofei Li^a, Peng Zhao^b, Qi Liu^a, Zhigang Yang^a, Hengjiang Cong^a, Hexiang Deng^a, Mingnan Chen^b, Shizhen Chen^c, Xin Zhou^c, Hong Ding^a, and Zhong-Xing Jiang^{a,d}

^aSchool of Pharmaceutical Sciences and College of Chemistry and Molecular Sciences, Wuhan University, Wuhan 430071, China

^bDepartment of Pharmaceutics and Pharmaceutical Chemistry, School of Pharmacy, University of Utah, Salt Lake City, Utah 84112, USA

^cState Key Laboratory for Magnetic Resonance and Atomic and Molecular Physics, Wuhan Institute of Physics and Mathematics, Chinese Academy of Sciences, Wuhan 430071, China

^dKey Laboratory of Synthetic Chemistry of Natural Substances, Shanghai Institute of Organic Chemistry, Chinese Academy of Sciences, Shanghai 200032, China

Abstract

Salinomycin is a promising anti-cancer agent which selectively targets cancer stem cells. To improve its potency and selectivity, an analogs library of salinomycin was generated by site-specific modification and CuAAC derivatization. Through a cytotoxicity analysis of the library, a fluorinated analog with high potency, selectivity, and ^{19}F MRI sensitivity was discovered as a novel theranostic agent.

Graphical Abstract



The first ^{19}F MRI sensitive theranostic agent was discovered through site-specific modification of salinomycin and click library derivatization.

Correspondence to: Zhong-Xing Jiang.

[†]Electronic Supplementary Information (ESI) available: Synthesis of library compounds, copies of ^1H NMR, ^{13}C NMR, ^{19}F NMR, IR and HRMS of compounds, and single-crystal X-ray diffractograms of $\mathbf{5f}\text{-Na}^+$ (CCDC 1448688) and $\mathbf{5f}\text{-K}^+$ (CCDC 1449564). See DOI: 10.1039/x0xx00000x

Salinomycin, a polyether ionophore antibiotic isolated from *Streptomyces albus*, has been commercially used in veterinary medicine for decades. In 2009, salinomycin was identified as a selective breast cancer stem cells inhibitor with activity 100-fold higher than paclitaxel.¹ Since then, its cytotoxicity against a variety of cancer stem cells and cancer cells has been discovered.² Although the detailed mechanism of these effects is still unclear,³ salinomycin is already in clinical trials for a panel of cancers. Therefore, generation of highly potent, highly specific salinomycin analogs is of great interest. Further, it is desired if the analogs can also be used to probe the modes of action of salinomycin.

As a complex natural product with 18 chiral centres, 5 rings, and multiple reactive groups, the site-specific modification of salinomycin is very challenging. Currently, the modification strategies are limited to esterification or amidation of its carboxylic group, acylation of its hydroxyl groups, and hydrogenation of its double bond (Fig. 1).⁴ Recently, Strand's group developed a strategy for site-specific acylation of the hydroxyl groups in salinomycin and found that C20-acylated analogs with the least bulky substituents had the highest potency against cancer cells.^{4f,5} The X-Ray crystal and molecular modelling of salinomycin show that the C20 hydroxyl group is not involved in ion chelation, and its acylation actually poses steric hindrance for ion chelation.⁶ We envisioned that the inversion of the C20 configuration could relieve the steric hindrance and therefore enhance ion chelation and potency. In this way, a highly valuable conjugation site is also available for targeted delivery of salinomycin without compromising its ion chelation and potency.⁷ To this end, inversion of the C20 hydroxyl group with an azido group is preferred because it could provide easy access to various salinomycin analogs and conjugates using the Cu-catalyzed azide-alkyne cycloaddition (CuAAC) reaction⁸ under mild conditions (Fig. 1). Herein, we report a convenient strategy for the C20-specific modification of salinomycin with an azido group and the consequent generation of a library of analogs through the CuAAC reaction, as well as a detailed cytotoxicity assay of the library.

After esterification of salinomycin **1** with TMS(CH₂)₂OH using a reversible strategy for carboxylic group masking (Scheme 1),^{4f} the selective inversion of the C20 configuration with an azido nucleophile was investigated. Because the allylic C20 hydroxyl group is more reactive than C9 and C28 ones,^{4f,6} selective tosylation of **2** provided C20 tosylate **S1** in high yield (See supporting Information). However, many attempts at nucleophilic substitution of the tosylate group with an azido group resulted in the decomposition of **S1**. Fortunately, an azido group was successfully introduced into **2** at C20 through the Mitsunobu reaction with diphenylphosphoryl azide (DPPA) as a nucleophile. Azide **3** was obtained with a 73% yield and no C9- or C28-substituted side product was isolated. Unmasking the carboxylic group with tetrabutylammonium fluoride (TBAF) provided the key intermediate **4** on a multi-gram scale with a 68% yield. To generate a diverse library of salinomycin analogs using the CuAAC reaction, a panel of 26 alkynes were selected, including 9 phenyl-containing, 6 nitrogen-containing, 7 hydroxyl-containing, and 4 ether-containing alkynes. As expected, each alkyne was conveniently coupled with azide **4**, respectively, in the presence of CuSO₄ and sodium ascorbate under mild conditions to give triazols **5a-z** with good yields.

To illustrate the structures of triazols **5a-z**, single-crystal X-ray structures of **5f**-Na⁺ and **5f**-K⁺ were obtained (Fig. 2). It was found that **5f** can adopt a suitable conformation to chelate

ions, Na⁺ or K⁺, with its oxygen atoms. As expected, the Mitsunobu reaction took place exclusively at C20 with the inversion of the configuration, and, consequently, the CuAAC reaction constructed a triazol sidearm which stretched out of the ion chelation pocket. In this way, both the steric effect and chelation perturbation of ion chelation were successfully avoided.

The cytotoxicity of these salinomycin analogs **5a-z** together with salinomycin **1** and azide **4** was then evaluated in 4T1 murine breast cancer cells using a MTT assay (Table 1). Surprisingly, azide **4** showed a 27-fold loss of potency as compared to salinomycin. Out of the library, all 9 phenyl-containing triazols **5a-i** displayed higher or comparable potency to salinomycin. These EC₅₀ values compare very favourable to bulky substituents without a hetero atom, which display EC₅₀ of 2.29–2.46 μM for **5b-d**. With the exception of 3-pyridine substituted **5k**, the EC₅₀ of 5 nitrogen-containing triazols **5j-o** were much higher than that of salinomycin. In these cases, the strong chelation ability of nitrogen may pose a perturbation on ion chelation.^{4f} The same trend was observed in the 7 hydroxyl-containing triazols **5p-v**. It is noteworthy that no significant cytotoxicity was observed for triazols **5t-v** with ethylene glycol units which are known to chelate ions. Among the 4 ether-containing triazols **5w-z**, perfluoro-*tert*-butyl ether **5w** turned out to be the most potent one with an EC₅₀ of 1.52 μM, which is over 2-fold more potent than salinomycin. Notably, perfluoro-*tert*-butyl is a bulky group ideal for ¹⁹F magnetic resonance imaging (¹⁹F MRI).⁹ Based on these observations, it is clear that bulky substituents on the C20 triazol is preferred for achieving high potency. In contrast, C20 hydroxyl acyl analogs with the least bulky substituent exhibited the highest potency.^{4f} Therefore, inversion of the C20 configuration indeed improves the potency.

Based on the initial assay, triazols **5b**, **5d**, **5k**, **5w** and salinomycin were selected for further assay on human cells (Table 2). Besides human hepatic cells (L02), a panel of cancer cells were selected, including human glioblastoma cells (U87), cervical cancer cells (Hela), epithelial colorectal adenocarcinoma cells (Caco2), and breast cancer cells (MCF-7). Compared to salinomycin, these triazols displayed dramatically lower cytotoxicity against normal L02 cells and significantly higher cytotoxicity towards cancer cells. For example, **5d**, **5k** and **5w** displayed over 2-fold higher cytotoxicity towards U87, and **5b** exhibited 2.9-fold higher cytotoxicity towards MCF-7 than that of salinomycin. It is noteworthy that, compared to salinomycin, **5w** showed 29.5-fold higher cytotoxicity towards Caco2 with an IC₅₀ of 0.44 μM.

To evaluate the clinical potential of triazols **5b**, **5d**, **5k**, and **5w**, the selectivity index (SI) was calculated with salinomycin as a comparison (Table 3). It is an indication of a drug with efficacy against cancer cells when SI > 1.0. For selected cancer cells, salinomycin showed a low SI except for in Hela cells. In contrast, these triazols had a significantly higher SI than salinomycin. For example, **5b** displayed the highest SI of 8.85 for Hela and **5d** displayed the highest SI of 5.89 for Caco2. Among these triazols, **5w** is very promising because it had high potency and SI for Hela and Caco2 cells.

With 9 symmetrical fluorine atoms, fluorinated triazol **5w** is also a valuable ¹⁹F NMR/MRI probe for better understanding the mechanism of salinomycin's selective cytotoxicity on

CSCs. In recent years, ^{19}F MRI has been widely used in tracking targets of interest¹⁰ and monitoring biological reactions.¹¹ Compared to other imaging technologies, ^{19}F MRI is able to provide high-contrast *in vivo* images without an endogenous background and ionizing radiation. Trizol **5w** gives a strong singlet ^{19}F NMR peak at -70.50 ppm from its nine symmetrical fluorines. Regardless of the size and chelation pattern of the ions, little chemical shift change was observed when **5w** was chelated with a panel of ions (Fig. 3a), which can dramatically simplify the downstream ^{19}F MRI study. ^{19}F MRI relaxation experiments indicated that **5w** has appropriate relaxation times for ^{19}F MRI with a longitudinal relaxation time T_1 of 843 ms and a transverse relaxation time T_2 of 445 ms. Then, a ^{19}F MRI phantom experiment of **5w** was carried out on an array of its solutions in DMSO. With a short scan time of 128 seconds, **5w** was imaged by ^{19}F MRI at a concentration as low as 1.1 mM (or 10 mM in ^{19}F concentration, Fig. 3b). Because of its high cytotoxicity, selectivity, and ^{19}F MRI sensitivity, **5w** is a promising ^{19}F MRI traceable mechanism probe for CSCs and a drug candidate for imaging-guided cancer therapy.

In summary, a fluorinated salinomycin analog with high potency and selectivity against cancer cells and high ^{19}F MRI sensitivity was discovered. The Mitsunobu reaction enables the site-specific modification of salinomycin with high efficacy, while the CuAAC reaction provides a convenient way to generate a salinomycin analog library under mild conditions. Importantly, inversion of the C20 configuration of salinomycin can relieve steric hindrance, enhance ion chelation, improve potency, and provide a valuable conjugation site for targeted delivery. The results presented here could serve as a starting point for the discovery of clinically useful salinomycin-based anti-cancer agents, ^{19}F NMR/MRI-guided mechanism study of salinomycin's effects on CSCs, and ^{19}F MRI-guided cancer therapy. Using the fluorinated salinomycin analog as a mechanism probe to study its modes of action on CSCs is currently in progress and will be published in due course.

Supplementary Material

Refer to Web version on PubMed Central for supplementary material.

Acknowledgments

We are thankful for financial support from the National Natural Science Foundation of China (21372181 and 21572168), the Key Laboratory of Synthetic Chemistry of Natural Substances (Shanghai Institute of Organic Chemistry), and the National Institutes of Health (R00CA153929).

Notes and references

1. Gupta PB, Onder TT, Jiang G, Tao K, Kuperwasser C, Weinberg RA, Lander ES. *Cell*. 2009; 138:645. [PubMed: 19682730]
2. (a) Tang QL, Zhao ZQ, Li JC, Liang Y, Yin JQ, Zou CY, Xie XB, Zeng YX, Shen JN, Kang T, Wang J. *Cancer Lett*. 2011; 311:113. [PubMed: 21835542] (b) Schenk M, Aykut B, Teske C, Geise NA, Weitz J, Welsch T. *Cancer Lett*. 2015; 358:161. [PubMed: 25529011]
3. (a) Huczy ski A. *Chem Biol Drug Des*. 2012; 79:235. [PubMed: 22145602] (b) Huczy ski A. *Bioorg Med Chem Lett*. 2012; 22:7002. [PubMed: 23063400]
4. (a) Huczy ski A, Janczak J, Stefa ska J, Antoszczak M, Brzezinski B. *Bioorg Med Chem Lett*. 2012; 22:4697. [PubMed: 22721714] (b) Huczy ski A, Janczak J, Antoszczak M, Wietrzyk J, Maj E, Brzezinski B. *Bioorg Med Chem Lett*. 2012; 22:7146. [PubMed: 23079523] (c) Antoszczak M,

- Maj E, Stefa ska J, Wietrzyk J, Janczak J, Brzezinski B, Huczy ski A. *Bioorg Med Chem Lett*. 2014; 24:1724. [PubMed: 24631190] (d) Antoszczak M, Popiel K, Stefa ska J, Wietrzyk J, Maj E, Janczak J, Michalska G, Brzezinski B, Huczy ski A. *Eur J Med Chem*. 2014; 76:435. [PubMed: 24602789] (e) Antoszczak M, Maj E, Napiorkowska A, Stefa ska J, Augustynowicz-Kopec E, Wietrzyk J, Janczak J, Brzezinski B, Huczy ski A. *Molecules*. 2014; 19:19435. [PubMed: 25429565] (f) Borgström B, Huang X, Pošta M, Hegardt C, Oredsson S, Strand D. *Chem Commun*. 2013; 49:9944.(g) Sprott, KML., Choi, H., Fang, F., Shan, M., Lazarova, TI., Li, L., Siddiqui, MA., Larouche-Gauthier, R., Lemire, A. US. 20140371285 A1. 2013.
5. (a) Miyazaki Y, Shibuya M, Sugawara H, Kawaguchi O, Hirsoe C. *J Antibiot*. 1974; 27:814. [PubMed: 4452657] (b) Miyazaki Y, Kinashi H, Otake N, Mitani M, Yamanishi T. *Agric Biol Chem*. 1976; 40:1633.(c) Hammann P, Raether W, Vertesy L. *J Antibiot*. 1993; 46:523. [PubMed: 8478273]
6. (a) Paulus EF, Kurz M, Matter H, Vértesy L. *J Am Chem Soc*. 1998; 120:8209.(b) Huang X, Borgström B, Månsson L, Persson L, Oredsson S, Hegardt C, Strand D. *ACS Chem Biol*. 2014; 9:1587. [PubMed: 24841425]
7. (a) Zhao P, Dong S, Bhattacharyya J, Chen M. *Mol Pharm*. 2014; 11:2703. [PubMed: 24960465] (b) Huczy ski A, Antoszczak M, Kleczewska N, Lewandowska M, Maj E, Stefa ska J, Wietrzyk J, Janczak J, Celewicz L. *Eur J Med Chem*. 2015; 93:33. [PubMed: 25644674] (c) Antoszczak M, Sobusiak M, Maj E, Wietrzyk J, Huczy ski A. *Bioorg Med Chem Lett*. 2015; 25:3511. [PubMed: 26163197]
8. Meldal M, Tornøe CW. *Chem Rev*. 2008; 108:2952. [PubMed: 18698735]
9. (a) Jiang ZX, Liu X, Jeong EK, Yu YB. *Angew Chem Int Ed*. 2009; 48:4755.(b) Jiang ZX, Yu YB. *J Org Chem*. 2010; 75:2044. [PubMed: 20170088]
10. (a) Ahrens ET, Flores R, Xu H, Morel PA. *Nat Biotechnol*. 2005; 23:983. [PubMed: 16041364] (b) Vivian D, Cheng K, Khuranan S, Xu S, Kriel EH, Dawson PA, Raufman JP, Polli JE. *Mol Pharmaceutics*. 2014; 11:1575.
11. (a) Mizukami S, Takikawa R, Sugihara F, Hori Y, Tochio H, Walchli M, Shirakawa M, Kikuchi K. *J Am Chem Soc*. 2008; 130:794. [PubMed: 18154336] (b) Bruemmer KJ, Merrikhihaghi S, Lollar CT, Morris SN, Bauer JH, Lippert AR. *Chem Commun*. 2014; 50:12311.

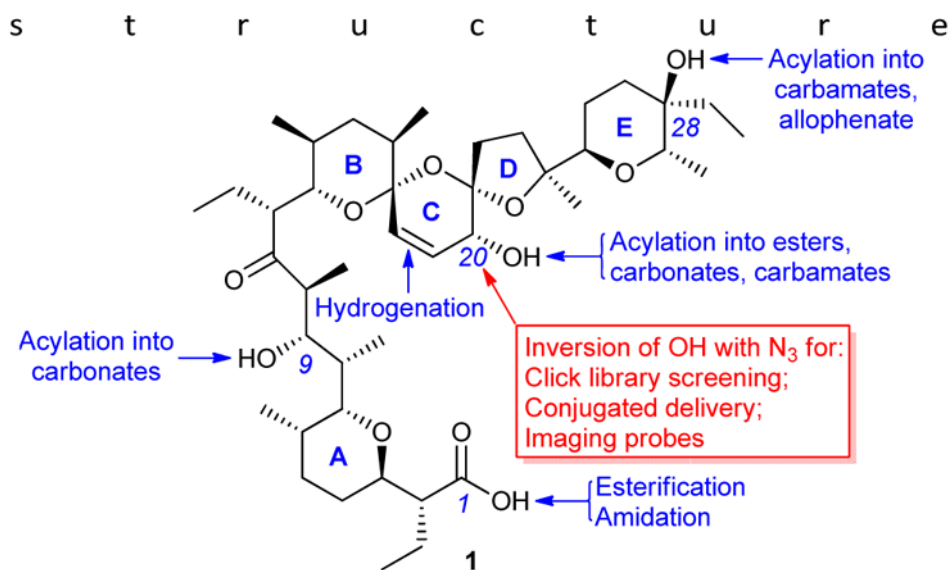


Fig. 1.
Methods for modification of salinomycin 1.

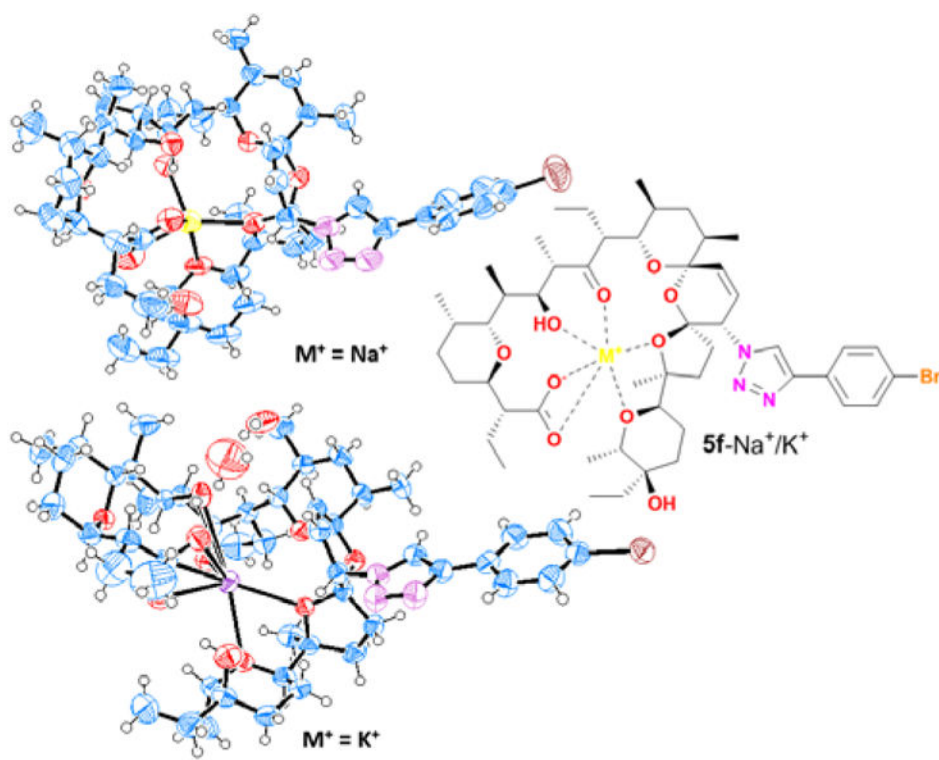


Fig. 2.
Single-crystal X-ray structures of $5f-Na^+$ and $5f-K^+$.

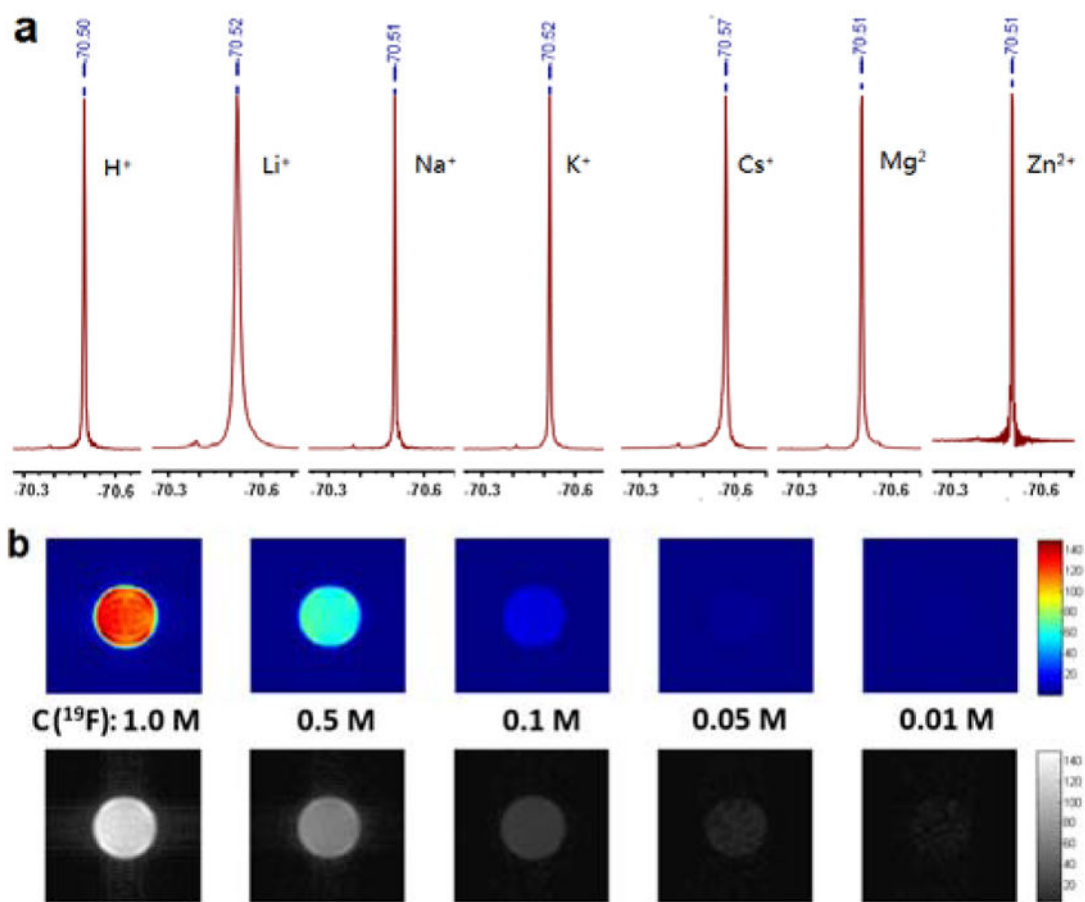
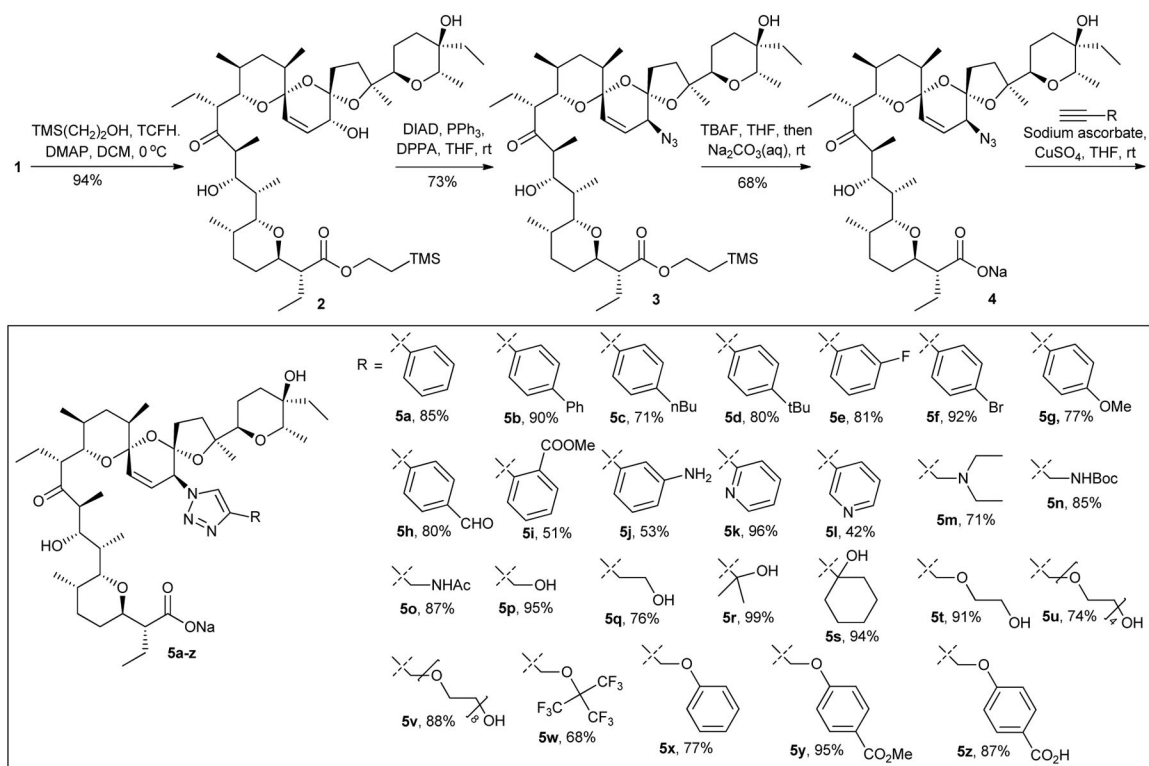


Fig. 3. (a) ^{19}F NMR of $5\mathbf{w}$ and its ion complexes. (b) ^{19}F MRI phantom images of $5\mathbf{w}$ (Upper: coloured; Lower: black-white).



Scheme 1.
Synthesis of salinomycin-based click library.

Table 1

EC₅₀ of salinomycin **1**, azide **4** and trizol **5a-z** on murine 4T1 cell.

Compd no.	EC ₅₀ (μM)	Compd no.	EC ₅₀ (μM)	Compd no.	EC ₅₀ (μM)
<i>Core compounds</i>					
1	3.42	5h	5.08	5q	20.44
		5i	3.83	5r	>>1000
4	95.20	<i>N-containing</i>		5s	8.80
<i>Ph-containing</i>					
5a	4.00	5j	13.37	5t	>>1000
5b	2.46	5k	2.91	5u	>>1000
		5l	7.02	5v	>>1000
5c	2.31	5m	23.14	<i>Ether-containing</i>	
5d	2.29	5n	9.97	5w	1.52
5e	3.33	5o	>>1000	5x	33.42
5f	3.69	<i>OH-containing</i>		5y	3.95
5g	3.07	5p	>>1000	5z	>>1000

Table 2

IC₅₀ of salinomycin **1**, analogs **5b**, **5d**, **5k** and **5w** on a panel of cells.

Compd no.	IC ₅₀ (μM)				
	L02	U87	Hela	Caco2	MCF-7
1	0.69	38.70	0.32	12.99	7.95
5b	2.96	50.02	0.33	1.29	2.75
5d	10.72	18.89	2.01	1.82	27.44
5k	3.52	15.74	0.61	3.31	8.87
5w	1.12	16.64	0.29	0.44	6.48

Table 3

Selectivity index (SI) of salinomycin **1**, triazols **5b**, **5d**, **5k** and **5w** on a panel of cancer cells over normal cell L02.

Compd no.	Selectivity index SI			
	U87	Hela	Caco2	MCF-7
1	0.02	2.16	0.05	0.09
5b	0.06	8.85	2.29	1.07
5d	0.57	5.33	5.89	0.39
5k	0.22	5.76	1.07	0.40
5w	0.07	3.82	2.57	0.17

The SI was calculated using formula: $SI = IC_{50}(L02)/IC_{50}(\text{cancer cell})$.